DOI: 10.1243/09576509JPE645

# Hydraulic air pumps for low head hydropower

**D.A. Howey[1] and K.R. Pullen[2] ***
1 Electrical Engineering Deptartment, Imperial College, Exhibition Road, South Kensington, London SW7 2AZ
2 School of Engineering and Mathematical Sciences, City University, Northampton Square, London EC1V 0HB
* corresponding author

## Abstract

Hydropower is a proven renewable energy resource and future expansion potential exists in smaller-scale, low-head sites. A novel approach to low-head hydropower at run-of-river and tidal estuary sites is to include an intermediate air transmission stage. Water is made to flow through a siphon, rather than a conventional water turbine, and at the top of the siphon the pressure is sub-atmospheric and air is entrained into the water. The siphon forms a novel hydraulically powered vacuum pump, or 'hydraulic air pump' (HAP). Air is pumped by the HAP through a separate air turbine and generator. This arrangement offers dramatic increases in turbine-generator speed and allows better control and matching of components and lifecycle cost reductions due to reduced maintenance costs and the use of smaller rotating machines.

This study builds on previous work on such systems by showing why the pumping process can be treated as isothermal. Also, initial test results with a small siphon are presented and compared to existing models. These show a discrepancy between predicted and measured pressure ratios and therefore an over-prediction of efficiency and power output using simple mathematical models.

**Keywords:** hydro-electric, hydro-power, tidal power, low-head, pneumatic transmission, renewable energy, hydraulic air compressor, hydraulic air pump, two phase diffuser, isothermal compressor

## 1. Introduction

Hydropower supplied 6.3% of the world's primary energy in 2006 [1]. This equates to almost a fifth of global electricity production. However, most large sites that can be exploited economically have already been developed [2]. Smaller sites are now sought, but lack of economies of scale means they are more expensive. Low head sites are the most widespread [2]. Various devices are used for energy extraction at low heads, including propeller turbines, cross flow turbines, water wheels and Archimedes screws. Another approach that has been explored is the hydraulic air pump (HAP) combined with an air turbine and generator. In this system, air is entrained into water at sub-atmospheric pressure using a siphon, with possible additional pressure recovery in a diffuser. The suction power pumps air through an air turbine and generator as shown in Figure 1.

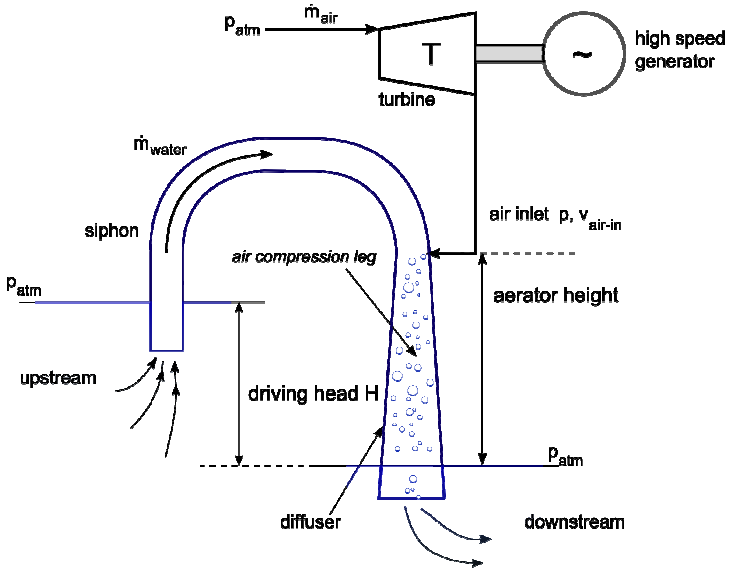


**Figure 1: Schematic diagram of HAP-turbine-generator system using siphon and diffuser**

Whilst the addition of an extra energy conversion stage seems cumbersome, the system may have the following advantages:

- lower cost of delivered power due to substantially smaller higher speed rotating machines for a given power output
- lower maintenance costs because there are no moving parts in the water
- easy regulation of power output and good component matching
- inherently fail-safe
- possible environmental benefits e.g. aeration of water, fish-friendliness
- ability to multiplex many siphons driving a single high power density air turbine/generator, either in parallel or in a series configuration (ie. at different downstream stations)

This system is unlikely to be appropriate at very small 'pico-hydropower' scales, below 5kW, because at these sizes there are significant disadvantages in using high speed turbo-machinery over directly coupled turbines and waterwheels. However, at larger sizes it will have advantages where there is a large volume flow rate of water but the head is only 0.5-2m. In order to be commercially viable, it is vital that the generating plant has a capacity as great as possible, but a single large direct-drive low head turbine or wheel becomes physically large and cumbersome above 50kW. This is therefore the market niche for the HAP system. However, for laboratory testing purposes, smaller scale prototype HAPs and turbine-generators may of course be used as long as scaling effects are carefully accounted for. An air turbine-generator, shown in Figure 2, was demonstrated both in the laboratory in the Mechanical Engineering Department at Imperial College London and connected to a HAP in a pilot plant at Grimsby Docks, Lincolnshire. This machine used a turbocharger turbine and 10kW, 60,000rpm axial flux permanent magnet generator with 150mm outer casing diameter. A set of variable angle nozzles were designed and mounted inside a specifically built aluminium alloy compressor volute. The variable nozzles allowed the turbine to be matched to the flow conditions which were uncertain until the time of testing of the HAP. The air turbine generator was tested using a high pressure ratio vacuum fan in the laboratory before dispatch to Grimsby Docks. Grimsby Docks was a useful testing site since tidal variation generates different water heads and the capacity of the dock means that the head can be held at a stable level for periods of large fractions of an hour. Unfortunately, further access to the test channel at the dock was stopped due to building work hence detailed tests on a small HAP were done in the laboratory as described later.

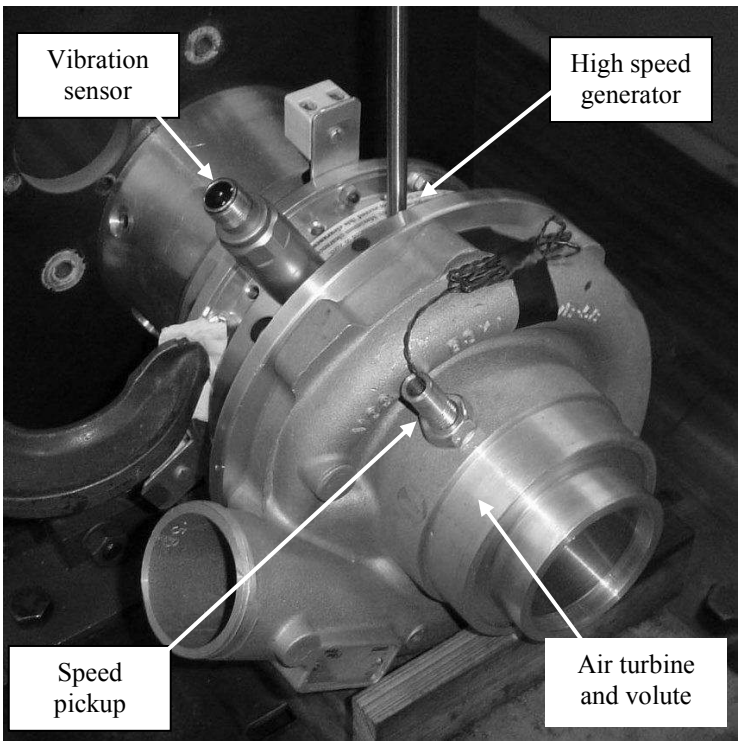


**Figure 2: 10kW, 60krpm air-turbine generator**

## 2. Literature review

Water power has been used for air compression for several hundred years. In Catalonia a device called a hydraulic 'trompe' was introduced in the 17th century for pressurising air prior to combustion in iron furnaces [3]. A similar device was used in North America for producing compressed air and there is a working example at Ragged Chute, Cobalt, Canada [4]. In North America this type of device was sometimes called a hydraulic air compressor (HAC) or Taylor compressor after Charles Taylor who patented his 1895 version [5]. In Taylor's device air is entrained into water flowing into a down pipe. As the two phase mixture descends, the pressure increases under the weight of the water, compressing the air. At the bottom of the down pipe, the mixture separates in a cavern. The water is then carried up a separate pipe to surface level. The head difference between the down-pipe entrance and up-pipe exit drives the system. The compressed air in the lower sump is available for whatever use is required. These HACs are capable of producing cool, dry compressed air with efficiencies from 40 to 85%. In 1901, Webber [5] demonstrated a system with a maximum measured efficiency of 71% (it is unclear whether isothermal or adiabatic efficiency is quoted), compressed air moisture content 20-30% of the atmospheric humidity level and air exit temperature equal to water temperature. Webber tested the system at different air/water mass flow ratios and used the HAC as a supercharger for a coal engine. He comments that the compressed air can be transmitted four miles with only a 2% pressure loss. Since there are no moving parts, maintenance levels are very low and there are reports of one system working almost maintenance free between 1910 and 1963 [4]. The disadvantage is the requirement for extensive civil works, hence the HAC cannot compete on capital cost with a comparable conventional compressor.

A variation is to use water to pump air *into* the system at sub-atmospheric pressures, rather than produce compressed air flowing *out* of the system at greater than atmospheric pressures. This avoids having to excavate a deep tunnel and cavern. Rather than using the term 'HAC' to describe this device, the term 'hydraulic air pump' or HAP shall be used henceforth to refer to this system, which is in essence a vacuum pump. The method of achieving this is with a siphon arrangement as illustrated in Figure 1. A diffuser can be added to recover kinetic energy. Water is raised above the inlet level before dropping to an outlet below. The static pressure drops according to conservation of energy in the raised section above the inlet because the potential energy increases but, in a constant diameter pipe, the average velocity cannot change because of continuity. Within the UK, work has been undertaken on HAPs at Coventry [6] and Lancaster [7] Universities. Bellamy [6] constructed a prototype which was tested in Derbyshire. The best measured water to air power efficiency was 25%, which was lower than the expected 50%. A reason for the discrepancy is not given.

A simplified analysis of a HAP is given by French and Widden [7] at Lancaster University. This analysis lumps together the loss terms and considers the water velocity through the siphon to be constant, allowing a direct analytical solution for the compression ratio. The approach is very helpful for understanding the system performance, and is used here with some clarification as a basis for comparison with experimental results.

No authors have published computational fluid dynamics (CFD) studies of HACs or HAPs. CFD could be a useful tool in gaining an understanding of qualitative aspects of two-phase flow in bubbly mixed regions such as bends. However, bubble formation, coalescence and breakup processes are not easily modelled/validated and therefore CFD should be approached with caution.

## 3. Analysis

### 3.1 Bubble heat transfer

In a HAP the air bubbles at entrainment are likely to be at temperatures below the water temperature since there is a temperature drop through the preceding air turbine. The length of time that the air requires to reach the water temperature is of concern. If the temperature increases within a short mixing distance, the analysis can proceed assuming isothermal compression. A thorough analysis of this transient heat transfer problem is complex, involving two phases and convection. However with simplifications a worst-case assessment can be made. The first approach would be to use the lumped capacitance method [8] where the bubble is treated as a solid with a spatially uniform internal temperature distribution. To test the validity of this method, the Biot number $Bi=[hr/(\lambda)]$ is calculated. The Biot number is the ratio between the surface heat transfer conductance and the internal heat transfer conductance. If $Bi >> 1$ then the internal thermal resistance dominates, whereas $Bi << 1$ implies that the surface thermal resistance dominates. In order to assume a uniform temperature distribution within the sphere, it needs to be shown that $Bi << 1$ [8]. For example $Bi < 0.1$ would imply an error less than

10% using the lumped capacitance assumption. Determining the convective heat transfer coefficient $h$ for the air-water surface is a problem. The value could lie for example between 50 and 10000 W/mK [8]. Nonetheless as Table 1 shows, a range of Biot numbers can be calculated for a typical bubble radius 2.5mm and assuming $\lambda_{air}$=0.026 W/mK (in practice $\lambda$ changes with temperature):

| **h (W/m$^2$K)** | 50 | 500 | 1000 | 5000 | 10000 |
|---|---|---|---|---|---|
| **Bi** | 4.81 | 48.1 | 96.2 | 481 | 962 |

**Table 1: Changes in Biot number with assumed convective heat transfer from 50 to 10000**

Based on these Biot numbers, the lumped capacitance method is not valid here and a two-dimensional calculation must be undertaken. By way of comparison, this is not the case for a similarly sized steel ball in water, where $Bi \approx 0.1$. To analyse accurately the temperature distribution within the bubble over time, radiation, conduction and convection should be considered in the air and water. However, considering internal conduction alone in both air and water is sufficient because it gives a worst case scenario (convection and radiation will improve the heat transfer rate). A numerical solution to the governing differential equations for conduction was obtained by discretizing in time and space using 5 nodes in space and 19 time steps, with the following assumptions:

- spherical bubble with no dissolution of air into water or vice versa and no phase changes
- air is dry and a perfect gas
- air-water boundary temperature is constant, equal to the water temperature
- bubble size is constant - therefore the bubble volume and density are constant; in practice this will not be the case
- convection and radiation are ignored and the temperature dependence of $c_p$, $\lambda$ and $\rho$ is ignored.

Slicing the sphere into concentric layers with a spherical core, as shown in Figure 3, with temperature nodes at the junctions, thermal resistance between adjacent nodes is calculated from Fourier's law in radial co-ordinates:

$$q = -\lambda \left(4\pi r^2\right) \frac{dT}{dr} \tag{1}$$

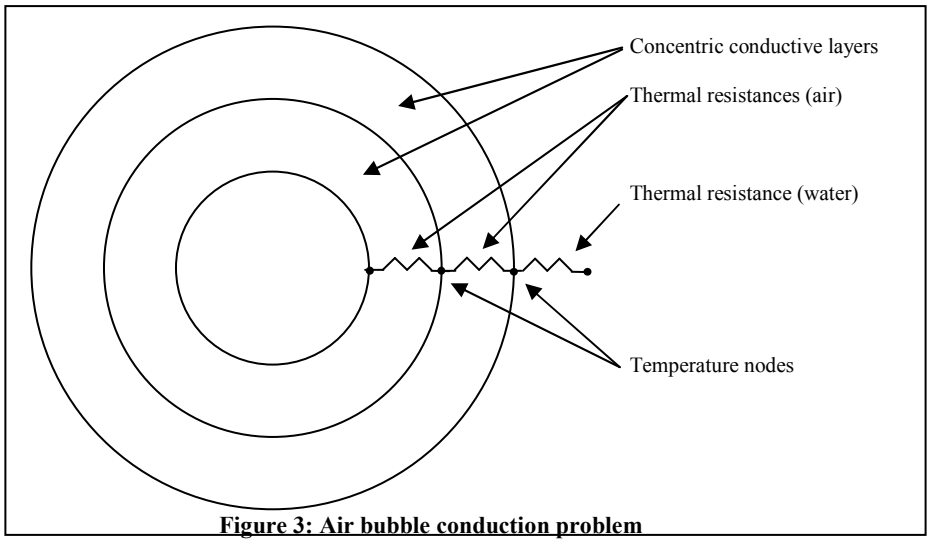


**Figure 3: Air bubble conduction problem**

At time t = 0, all node temperatures are set to initial values for the air and the water. The heat flux between adjacent nodes is calculated within a given time step using the above equation and the temperatures are then updated for the next time step by applying conservation of energy, with the boundary condition that the outermost water temperature is held at the initial water temperature. This is a reasonable assumption given the much greater heat capacity and conductivity of water compared to air. If the chosen time step size is too large the numerical solution becomes unstable and the temperatures do not converge as expected.

With a typical bubble size of 2.5mm diameter, and assuming a heat capacity for air between $c_p$ and $c_v$, 850 J/kgK, and $\lambda_{air}$ as above, Figure 4 shows the temperature evolution within the bubble over time, from a starting temperature of 240K with surrounding water temperature of 300K.

It can be shown that the difference between the innermost bubble node air temperature and the water temperature is less than 3K within 0.04s. At a typical water velocity of 2m/s this corresponds to a bubble travel distance of less than 8cm. The situation is similar for larger bubbles and for reasonable variations in the other parameters, as shown in Table 2. Note these are all worst case scenarios. In practice convection heat transfer will improve heat transfer rates.

| **Bubble radius** | **Initial innermost bubble node air-water temperature difference, ΔT [K]** | | | | |
|---|---|---|---|---|---|
| **[mm]** | **10** | **30** | **50** | **70** | **90** |
| **1** | 4 | 7 | 8 | 9 | 9.5 |
| **2.5** | 26 | 42 | 50 | 55 | 60 |
| **5** | 104 | 168 | 198 | 220 | 240 |

**Table 2: Distance travelled [mm] in 2m/s water before innermost bubble node temperature is within 3K of water temperature**

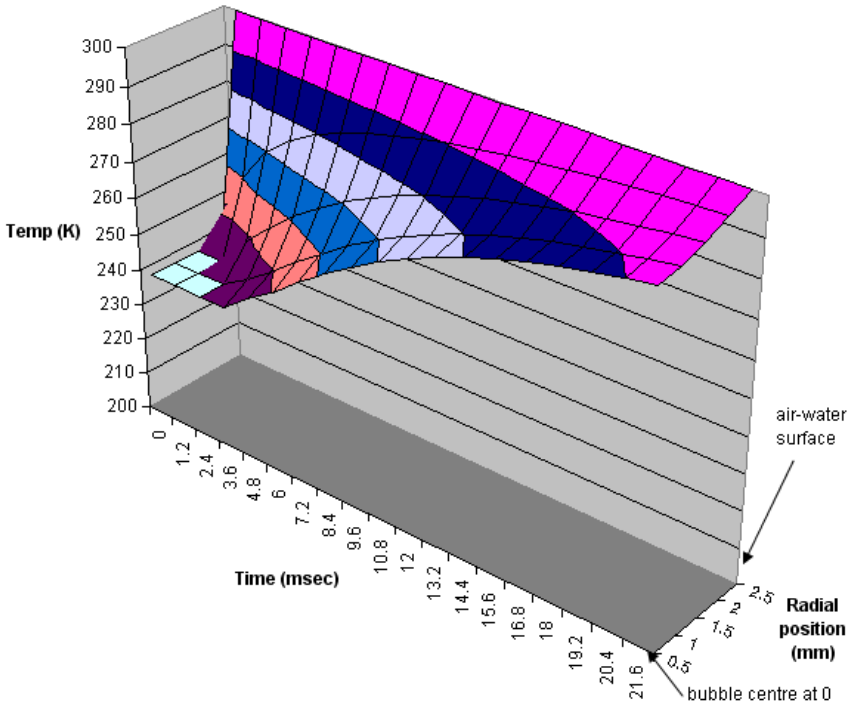


**Figure 4: Bubble heat transfer numerical solution for 2.5mm bubble, initial ΔT = 60K**

On this basis it can be assumed that HACs and HAPs are isothermal devices. Combined with a turbine an interesting thermodynamic cycle results, shown in Figure 5 . There is potential for 'reheat' at turbine inlet and refrigeration/cooling between stations 2 and 3.

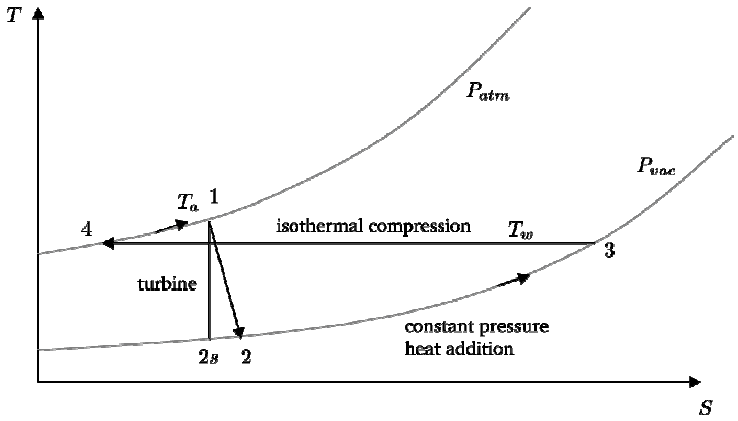


**Key**
1. At air intake prior to turbine
2s. Condition of isentropic expansion
2. Actual expansion through turbine
3. At air inlet to HAP
4. At HAP air outlet (atmospheric)

*Note:* it is assumed $T_{water} < T_{amb}$

**Figure 5: T-s diagram of proposed HAP thermodynamic cycle. Station numbers are also shown in Figure 1.**

### 3.2 System performance

Overall work input required to compress air isothermally is given by:

$$\dot{W}_{c\,iso} = \dot{m} \int \frac{dp}{\rho} = \dot{m}RT \int \frac{dp}{p} = \dot{m}RTln(r) \tag{2}$$

Compared to work required to compress air (assumed perfect gas, constant $c_p$) adiabatically and isentropically:

$$\dot{W}_{c\,ad} = \dot{m}c_p T_{lower} \left[ r^{\frac{\gamma-1}{\gamma}} - 1 \right] = \dot{m}c_p T_{upper} \left[ 1 - r^{\frac{1-\gamma}{\gamma}} \right] \tag{3}$$

At any pressure ratio, less work is required to compress air if the compression process is isothermal rather than adiabatic. This is clearly seen if a graph is plotted showing on the y-axis, the ratio of isothermal to adiabatic compression work (equation 2 divided by equation 3) for a given air flow and temperature, versus the pressure ratio on the x-axis. However, at the pressure ratios being investigated ($r_{max} \approx 2$) the difference is small ($W_{c\ iso}/W_{c\ ad} \approx 0.9$ ) [9]. Since a turbine is approximately adiabatic, a turbine connected to a HAP may be able to extract more work than the work required to pump/compress the air. This seems counterintuitive, but the reason for the discrepancy is that there is heat addition between the turbine outlet and start of compression process. If this is included then conservation of energy is maintained.

Efficiency can be defined in various ways. On a component level, for example for comparison of different HAP designs, the ideal efficiency is the isothermal air power divided by the water power:

$$\eta_{isoth} = \frac{\dot{m}_a RTln(r)}{\dot{m}_w gH} \tag{4}$$

This provides a comparison point for HAP designs. On a system level (i.e. considering turbine as well as HAP), the ideal efficiency is isentropic turbine air power divided by water power:

$$\eta_{isen} = \frac{\dot{m}_a c_p T_{inlet} \left[ 1 - r^{\frac{1-\gamma}{\gamma}} \right]}{\dot{m}_w gH} \tag{5}$$

Using the methods described by French and Widden [7], an analytical model has been developed to enable rapid on and off design point calculations for both of these configurations either separately or in combination. The model is a 1D steady state approach based on the drift-flux model for two-phase flow, where the phases share the same pressure field but have different velocity fields [10, 11].

### 3.3 HAP model

French and Widden [7] show by integrating the pressure change in the siphon downleg that:

$$\rho_w g y_1 = (p_2 - p_1) + x_1 p_1 ln(r) = (p_2 - p_1) + x_1\ p_2 \frac{1}{r} ln(r) \tag{6}$$

The method assumes the system is isothermal and that the bubble drift velocity is constant. Note that the term $x_1\ p_2\ [1/r]\ ln\ (r)$ gives the *buoyancy head*, or that part of the driving pressure which is used to compress the air; $x_1$ is the volumetric air-water ratio at inlet.

If the air and water velocities are equal then at a given point, $x = [(Q_a)/(Q_w)]$ where $Q$ is the volumetric flow rate of air or water. However, in a real system this is not the case; there is a slip velocity $v_r$ between the air and water because of the bubble buoyancy. French and Widden [7] discuss this in a general discussion of efficiency but do not explicitly show the slip loss term in their overall energy balance equation. The slip loss is defined as follows:

$$x = \left( \frac{Q_a}{Q_w} \right) \left( \frac{v_w}{v_a} \right) = \left( \frac{Q_a}{Q_w} \right) \left( \frac{v_w}{v_w - v_r} \right) \tag{7}$$

French and Widden [7] derive an overall energy balance expression which includes lumped loss terms for friction and bend losses, obtaining (in terms of driving head):

$$H = k_{losses} \frac{v^2}{2g} + x_1 \left[ \frac{1}{r} ln(r) \right] \frac{p_2}{\rho_w g} \tag{8}$$

This shows how the driving head is equal to the losses plus the buoyancy head. To obtain efficient operation, water speed $v$ should be kept at an optimum and $Q_a/Q_w$ increased to the maximum possible value without de-priming the siphon. If equations 7 and 8 are combined the following equation results:

$$H = k_{losses}\frac{v^2}{2g} + \left(\frac{Q_a}{Q_w}\right)_1 \left(\frac{v}{v - v_r}\right)\left[\frac{1}{r}ln(r)\right]\frac{p_2}{\rho_w g} \tag{9}$$

As the slip velocity increases, the fraction $[v/(v–v_r)]$ increases and this represents an increased loss. Equation 9 can be rearranged to obtain a relation between driving power, losses and air power. The resulting air power term is similar to the expression in equation 2 but with the slip loss included:

$$\dot{m}_w gH = \dot{m}_w k_{losses}\frac{v^2}{2} + \dot{m}_a RT\left(\frac{v}{v - v_r}\right)ln(r) \tag{10}$$

In equations 6, 8 and 9 the buoyancy head is expressed in a form that includes an additional term, $[1/r]$. This is because of algebraic manipulation so that $p_2$ appears explicitly rather than $p_1$. If the system is arranged for a vacuum, $p_2$ is atmospheric, whereas if it is arranged to produce compressed air at greater than atmospheric pressure, $p_1$ is atmospheric. The additional $[1/r]$ term leads to the interesting result that for the vacuum configuration there is a maximum attainable value of $[1/r]$ $ln$ $(r)$ when $r = e$ and therefore a maximum attainable value of buoyancy head. Taking $p_2$ as 100kPa and assuming the maximum value of air water volume-ratio whilst still remaining in the bubbly flow region [11], $x_1 = 0.3$ in equation 6, the maximum buoyancy head is 1.1m. For higher driving heads, HAP efficiency will necessarily drop.

A more complex HAP model can be developed assuming velocity and pressure both change throughout the system, but still with constant temperature. This gives more accurate results but loses the simplicity and clarity of the above analysis. The procedure is outlined in Rice and Bidini et al [12, 13].

### 3.4 Diffuser design

If a diffuser is included in the HAP downleg, the resulting flow is not uniform and empirical data must be used either across the whole diffuser or in discrete slices. Diffuser behaviour is difficult to predict because the flow is a two phase mixture. Research on single phase diffusers [14, 15, 16] shows that the optimal diffuser included angle for efficient pressure recovery in a single phase flow is 6–7°. Pressure recovery is usually measured using a pressure recovery coefficient for the whole diffuser (normalised to inlet dynamic pressure):

$$C_T = \frac{p_{out} - p_{in}}{0.5\rho_{mix}v_{in}^2} \tag{11}$$

Sometimes a correction factor is applied because the diffuser exit area is finite and therefore the flow exit speed is finite. However if exit dynamic pressure is much smaller than inlet, the above equation is valid.

Owen et al [17] conducted experiments on a horizontal conical diffuser with two phase flow gas void fractions $\alpha_a$ from 0 to 0.35, included angles 5–11° and area ratio 1:9. Various expressions for pressure recovery are derived but in practice it was found that an expression similar to equation 11 was adequate. The optimum included angle when diffusing an air-water flow with void fraction up to 0.35 was shown to be 7° , which is the same as with a single phase diffuser. In addition it was found that most pressure recovery was complete at the point where $[L/D] > 10–15$ (where $L$ is the diffuser length and $D$ the throat diameter), and that pressure recovery improved with increased upstream pressure. The authors measured $C_T$ of 0.5-0.85 using a 7º diffuser on a two-phase air-water mixture with void fractions of 0-30% at an upstream static pressure of 1.56 bar abs. As void fraction increased, $C_T$ decreased. The reason suggested is increased turbulence and flow separation in the two-phase flow. Neve [18] also identifies this and suggests that the decrease in pressure recovery with increased void fraction is caused by non-uniformity of density in the diffuser, because liquid is pulled toward the centre and gas toward the walls due to streamline curvature. This hypothesis seems plausible and the density non-uniformity described can clearly be seen in the experimental results of Thang and Davis [19].

Pressure recovery $C_T$ is a function of diffuser total angle, length, air inlet void fraction and upstream pressure:

$$C_T = f\left(\phi, L, \alpha_{air}, p_{up}\right) \tag{12}$$

For a horizontal diffuser, the pressure at diffuser exit is modelled completely by:

$$p_{out} = p_{in} + C_T 0.5 \rho_{mix\ in} v_{in}^2 - 0.5 \rho_{mix\ out} v_{out}^2 \quad (13)$$

The value of $C_T$ for different void fractions and upstream pressures must be found experimentally and stored; lookup tables can then be used in the computer model. Owen et al [17] give values of $C_T$ for different void fractions but these can only be used with caution since higher upstream pressures were used in their experiments than are used in low head hydropower.

In the case of a vertical diffuser with downwards flow, the situation is complicated by the hydrostatic pressure increase down the diffuser. The mixture density is dependent on the local static pressure and therefore increases down the diffuser and so instantaneous pressure recovery *dp* will improve down the diffuser because of the increase in local $\rho_{mix}$ and also the increase in $C_T$ with decreasing void fraction. For an accurate estimate of complete pressure recovery, the diffuser needs to be discretized into slices and $C_T$ updated at each slice, in conjunction with the compression calculation from the hydrostatic increase. However, a conservative estimate of performance can be made by separating the processes (dynamic pressure change, and hydrostatic increase) and adding together the results. The pressure increase from the siphon is calculated as if there were no change in pipe cross-sectional area, and then an additional pressure increase is added for the diffuser, as if the diffuser were horizontal, with $C_T$, $\rho_{mix\ in}$ and $v_{in}$ used to calculate the increase.

### 3.5 Summary and discussion of analytical results

HAP performance can be quantified in terms of efficiency and specific air pumping power. There are four parameters which greatly influence the performance and these are (1) driving head *H*, (2) inlet air-water volumetric ratio *x*, (3) loss coefficient *k* and (4) aerator height $y_1$. The driving head is constrained by geometry and the available water flow rate at the site where the HAP will be installed. The inlet air-water volumetric ratio should be chosen to be as high as possible without depriming the siphon. Other authors [7, 10] suggest a maximum value $x_{max} \approx 0.35$; in practice one might operate at a lower value such as x = 0.20 since siphon repriming is time consuming and should be avoided. The loss coefficients should be chosen to be as small as possible, although performance is less sensitive to this than might be expected. The aerator height should be chosen to be as large as possible but is limited by aesthetics, site constraints and the risk of cavitation. The sensitivity of efficiency and pumping power to these four parameters will now be investigated and summarised.

Figure 6 shows the sensitivity of isothermal efficiency to variations in *k* for a driving head of 1m, for two different scenarios. The first scenario is a maximum efficiency case, corresponding to a large aerator height and higher pressure ratio ($r \approx 2$), and the second scenario a maximum power case with a smaller aerator height, lower efficiency and lower pressure ratio ($r \approx 1.4$). Figure 6 gives predicted efficiencies for *families* of siphon devices, i.e. each data point actually implies a different design, which may or may not be practically achievable.

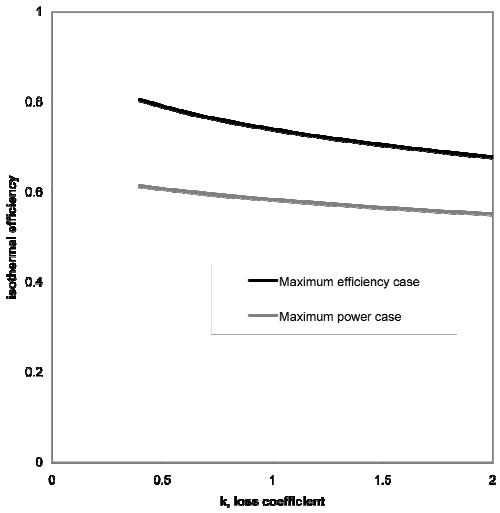


**Figure 6: Predicted maximum isothermal efficiency for a family of HAPs where aerator height is always chosen to give optimum efficiency or optimum power, with variations in loss factor k, assuming bubble drift velocity 0.25m/s, air-water volumetric ratio at air inlet 0.2 and head 1m.**

For a single efficient design at a fixed aerator height of 5m, the efficiency sensitivity to head and *k* is shown in Figure 7. Efficiency is sensitive to head. Driving heads above the maximum possible buoyancy head result only in higher water velocities, giving increased air power for a fixed volumetric ratio of air to water, but not improved pressure ratios. If a diffuser is employed, this can be understood as having the effect of lowering the lumped loss coefficient *k* by a value between 0 (for no diffuser) and 1 (for complete, and theoretically impossible, diffusion). However, referring to equation 8, lowering *k* by inclusion of a diffuser will increase the overall water velocity and therefore increase the air power for a given air-water volume ratio, Figure 8. The pressure ratio and efficiency however will be largely unchanged since they are governed primarily by driving head, aerator height and air-water volume ratio.

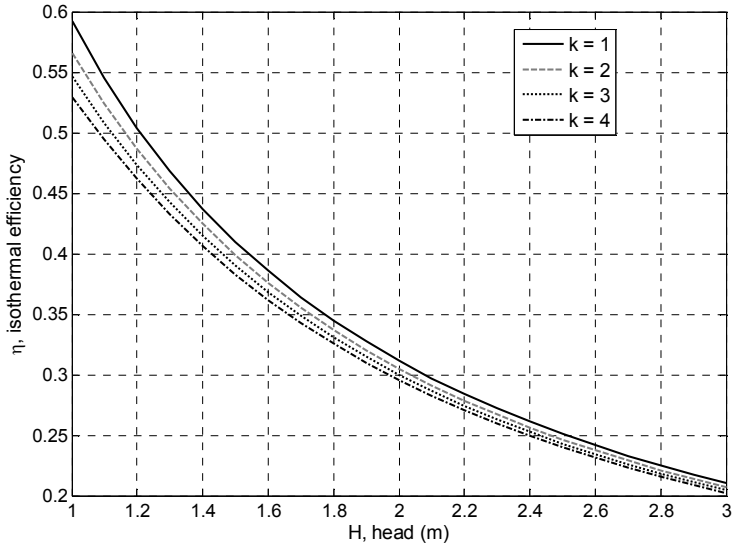


**Figure 7: Predicted isothermal efficiency for a single HAP with fixed aerator height 5m, showing sensitivity to loss factor k and head, assuming bubble drift velocity 0.25m/s, air-water volume ratio 0.2 at air inlet.**

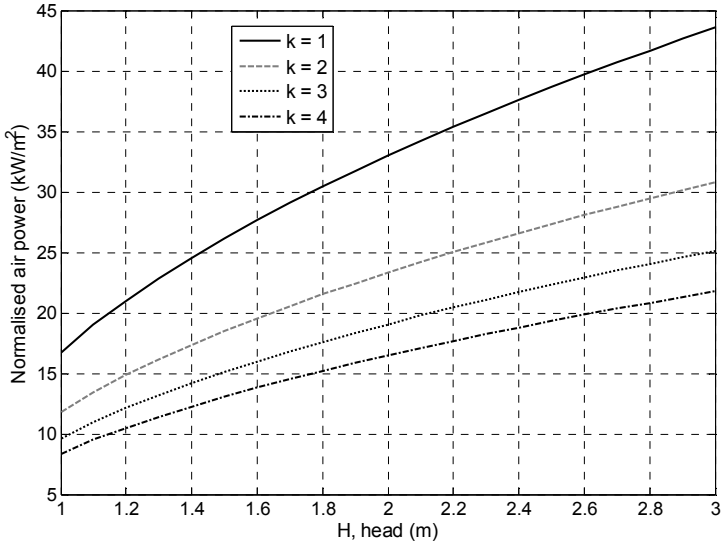


**Figure 8: Predicted air power (kW per $m^2$ cross sectional area of pipe) for a single HAP with fixed aerator height 5m, showing sensitivity to loss factor k and head, assuming bubble drift velocity 0.25m/s, air-water volume ratio 0.2 at air inlet.**

In summary, efficient operation is *only* achieved with a high aerator, giving a high pressure ratio, and with inlet air-water volume ratio as high as possible, and driving head near to maximum buoyancy head value. Loss coefficients and diffuser pressure recovery coefficient affect the air power achieved but have little effect on

efficiency. Practical limits on aerator height and inlet air-water volume ratio include cavitation due to low pressure at the top of the siphon, and siphon deprime due to excessive air flow into the siphon. If the air is not evenly distributed in the water at the aerator this may also lead to depriming. Therefore the aerator design is of great importance.

We suggest that Bellamy's [6] tests proved disappointing because not only was it difficult to achieve a uniform air-water mixture distribution, but also the system was not designed for a high aerator. Pictures of the test system indicate that the aerator height was not significantly above the upstream level – perhaps less than 1m higher. This would limit efficiency to approximately 20% and is indeed what was found in the tests, despite the inclusion of a venturi nozzle and diffuser in the device. As explained, a diffuser chiefly increases air power, not efficiency. The nozzle section has little effect because it is equivalent to simply having a smaller diameter pipe preceding the diffuser, albeit with slightly lower friction losses in this portion of the pipe system.

# 4. Experiment

### 4.1 Experimental arrangements

Experiments were conducted on the HAP shown in Figure 9 and Figure 10, using an existing tank arrangement to provide a head difference across the siphon. The HAP inner diameter was constant 100mm. The upper tank was 1x1x1m and the lower tank, located below floor level, measured 2x1x1m. A BOC-Edwards vacuum pump was used to prime the siphon. Due to the lack of available clearance between the upper tank and the lab ceiling in the test facility, only a modest aerator height could be achieved: 1.415m from aerator to base of upper tank, plus the distance from the lower water level to the base of the upper tank, which varied from 0.82 to 0.92m, giving a total aerator height of 2.235 to 2.335m. This was deemed acceptable. Air was entrained into the water at 8 holes each Ø6mm spaced equally on the outer edge of a transparent PVC pipe, having passed through a Cole-Parmer mass flow meter, valve and manifold.

Unfortunately the existing variable speed pump in the test rig had seized and therefore a fixed-speed submersible hire pump had to be used. This severely limited the ability to control driving head, but nonetheless meaningful results were achieved. Pressure measurements were taken using static pressure tappings connected to Druck PTX1400 4-20mA (0-1 bar) electronic pressure sensors located at the same height as each tapping. Water mass flow rate was measured using a calibrated bell-mouth entry and a pressure tapping within the bell-mouth at diameter 113mm. Head was measured by sight using a rule to measure upper and lower tank levels. At each steady state point, repeated measurements were taken and averaged. Temperature measurements were taken using thermocouples.

**Figure 9: Photograph of siphon rig, showing aerator**

The uncertainties in each measurement were as follows:

| | | |
|---|---|---|
| Air volume flow rate | ± 0.5 | LPM (litres per minute) |
| Pressure | ± 250 | Pa |
| Temperature | ± 1 | K |
| Head | ± 50 | mm |

**Table 3: Measurement uncertainties**

From these, the uncertainties in the final measurements of air and water mass flow, pressure, power, efficiency and so on were calculated using standard compound uncertainty analysis methods.

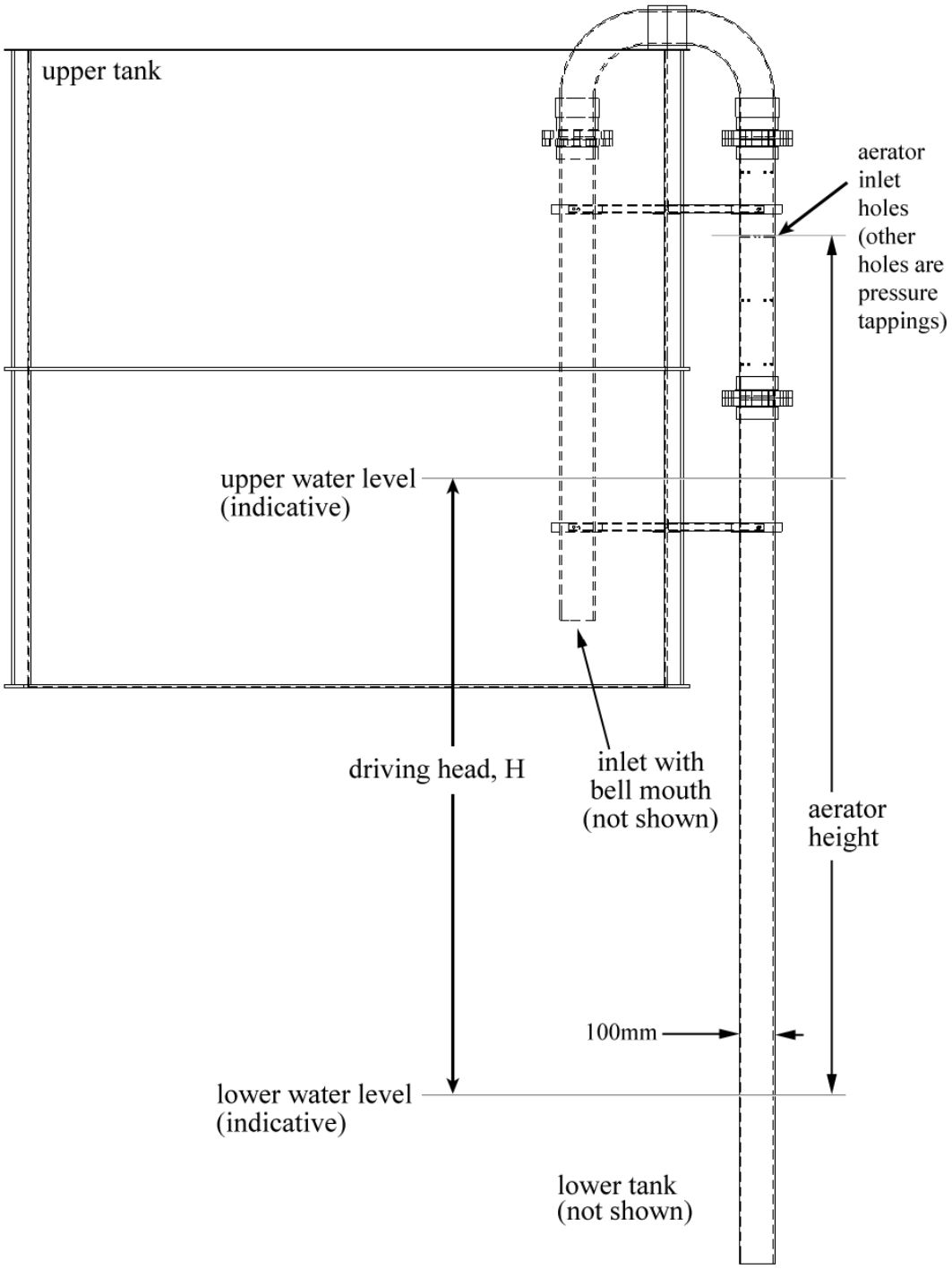


**Figure 10: Diagram showing experimental arrangement**

### 4.2 Results

Figure 11 shows the normalised results from the tests and also the model predicted results for comparison purposes. Uncertainty bars and fitted trend curves are shown. Horizontal uncertainty bars have been removed for clarity but it should be born in mind that there is considerable horizontal uncertainty at higher air-water mass ratios. Ideally each set of tests would have been conducted at a fixed head, but unfortunately due to the rig pump replacement, there was a lack of fine control of head. Therefore data was collected at various heads, from 1.16m to 1.54m. The water mass flow rates were then normalised by dividing each value by the head corresponding to each point. The x-axis shows the ratio between the air mass flow rate and this normalised water mass flow rate. Note that this is not a non-dimensional quantity but has units of metres because of the division by head. This normalisation assumes that water mass flow varies linearly with head and that water mass flow rate equals zero when head equals zero. Analysis of the raw data shows that the assumption of linearity is valid. The ambient temperature was recorded and used to calculate the air density and volume flow rate at inlet.

In order to generate the analytical results, the experimental conditions for air and water mass flow, head, loss factor (measured and found to be $k = 2.35$ for this rig) and aerator height were used in the analytical model to calculate predicted pressure ratio, assuming a constant bubble drift velocity of 0.25 m/s [7]. The pressure ratio was used to calculate isothermal efficiency and air power.

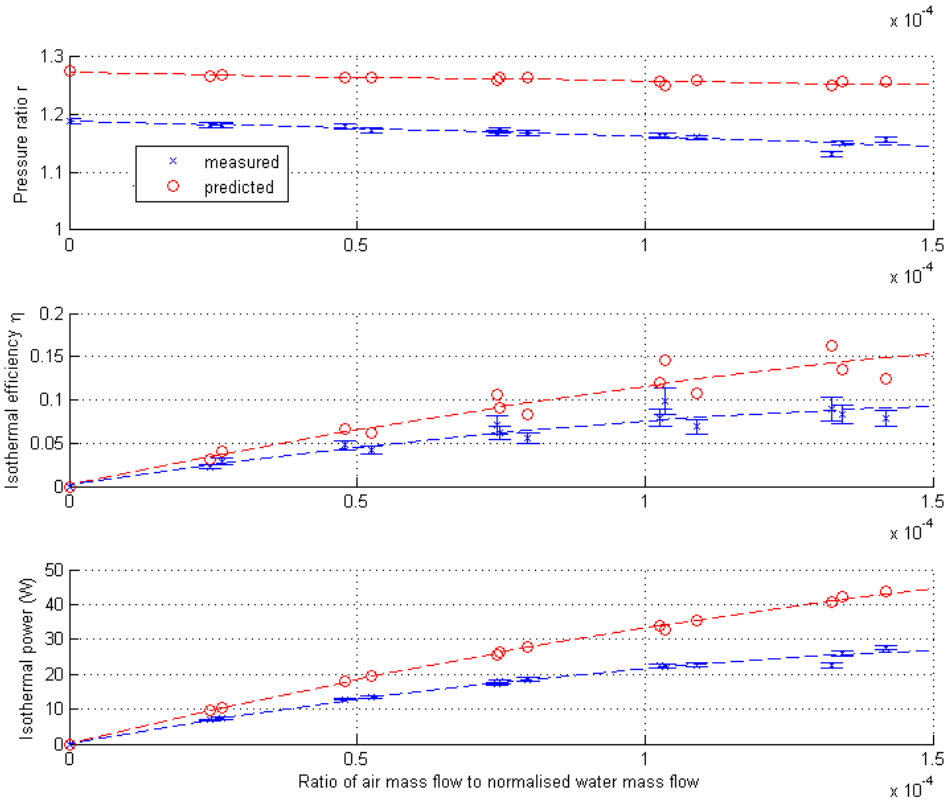


**Figure 11: Predicted and measured results for a range of airflows.**

## 5. Discussion

As can be seen from Figure 11, there is a discrepancy of 7-10% between predicted and actual pressure ratios, although general trends agree. This therefore leads to a discrepancy in calculated isothermal power and efficiency. Because air power depends on the natural logarithm of the pressure ratio, the air power and isothermal efficiency are very sensitive to discrepancies in pressure ratio, for example an 8% relative discrepancy in $r$ leads directly to a 42% relative discrepancy in isothermal efficiency.

The following reasons are suggested as to why the pressure ratio discrepancies were 7-10%:

1. Due to the unsteady nature of the two-phase pipe flow, the pressure readings fluctuated considerably during measurement. There may also have been problems with the pressure tappings themselves causing some additional pressure drop in the pipe.

2. Pressure drop across the air inlet and through the aeration process was not included in the model. Due to the complex two-phase nature of the mixing, finding relevant loss coefficients in the literature is difficult, and therefore this pressure drop is unknown at present.

3. The assumption of constant lumped loss factor $k$ (calculated using the zero airflow conditions) for all operating conditions may be invalid.

# 6. Conclusions

The authors believe that the measured efficiencies presented here are low principally because the siphon height was limited by the available roof height in the test facility. With a higher siphon, much higher efficiencies could be achieved under certain operating conditions – as indicated in the analysis of the theoretical model developed by French and Widden [7]. Therefore it is concluded that the HAP-based low head hydro-power system deserves further investigation as a low head, large volume flow technology for small hydro-power applications.

Experimental test data for HAP systems is limited but the analysis given here explains the poor results achieved by Bellamy [6]. The experiments conducted by the authors described in sections 4 and 5 show the HAP principle is operating as expected, although performance was weaker than predicted because of discrepancies between measured and predicted pressure ratios, to which the isothermal efficiency is very sensitive.

For simplicity and ease of manufacture, future experiments should probably be conducted using a closed piping system (rather than open tanks) with an appropriate air separator. A variable speed pump with feedback control is required to maintain a constant head across the siphon. This will allow for better comparison of results. In addition, a higher siphon with various aeration points and the option of including a diffuser will allow the performance variation with aerator height and diffusion to be investigated in detail. Finally, it is very important that pressure ratio is measured as accurately as possible.

# 7. Acknowledgements

The assistance of Dr Naill McGlashan, Mr Zhifeng Lim and Mr Chee Lee in constructing and operating the experiment is gratefully acknowledged. This research was funded by a grant from the Hadley Trust.

# 8. References

[1] **BP plc.** *BP Statistical Review of World Energy 2007*. BP, 2007, available at www.bp.com

[2] **International Energy Agency**. *World Energy Outlook 2002, 2nd Edition*. IEA Publications, 2002.

[3] **Estanislau, T.** The Catalan process for the direct production of malleable iron and its spread to Europe and the Americas. *Contributions to Science*, 1999, 1(2): 225-232.

[4] **Compressed Air Magazine**. An operating Taylor Hydraulic Compressor. *Compressed Air Magazine*, October 1963:24-25

[5] **Webber, W. O.** Test of an hydraulic air compressor. *Transactions of the American Society of Mechanical Engineers*, XXII, 1901.

[6] **Bellamy, N.W.** The Syfogen low head pneumatic hydro-electric system. In *Proceedings of the Conference on Hydropower into the Next Century*, 1995:563-570.

[7] **French, M.J. and Widden, M.B.** The exploitation of low-head hydropower by pressure interchange with air, using siphons. *Proceedings of the Institution of Mechanical Engineers. Part A, Journal of power and energy*, 2001, 215 (2): 223-230

[8] **Incropera, F.P., DeWitt, D.P., Bergman, T.L. and Lavine, A.S.** *Fundamentals of Heat and Mass Transfer*, 6th Edition, John Wiley and Sons, Inc., 2007.

[9] **Ayers, D.L**. Efficient hydraulic air compression for base loaded combustion turbines. In *The American Power Conference*, pages 406-412, 1991.

[10] **Wallis, G.B.** *One Dimensional Two-Phase Flow*. McGraw Hill Higher Education, 1969.

[11] **Whalley, P.B.** *Two-phase Flow and Heat Transfer*. Oxford University Press, 1996.

[12] **Rice, W.** Performance of hydraulic gas compressor. *Trans. ASME, J. Fluids Engng,* 1976, 96: 645-653.

[13] **Bidini, G., Grimaldi, C. N. and Postrioti, L.** Performance analysis of a hydraulic air compressor. *Proceedings of the Institution of Mechanical Engineers - A*, 1999, 213 (3): 191-204.

[14] **Engineering Sciences Data Unit**. Performance improvement of axial diffusers for incompressible flow. *EDSU Data Sheet number 87015*, 2006a.

[15] **Engineering Sciences Data Unit**. Introduction to design and performance data for diffusers. *EDSU Data Sheet number 76027*, 2006b.

[16] **Engineering Sciences Data Unit**. Performance of conical diffusers in incompressible flow. *EDSU Data Sheet number 73024*, 2004.

[17] **Owen, I., Abdul-Gani, A. and Amini, A.M.** Diffusing a homogenized two-phase flow. *International Journal of Multiphase Flow*, 1992, 18 (4): 531-540.

[18] **Neve, R.S.** Diffuser performance in two-phase jet pumps. *International Journal of Multiphase Flow*, 1991, 17 (2): 267-272.

[19] **Thang, N.T. and Davis, M.R.** The structure of bubbly flow through venturis. *International Journal of Multiphase Flow*, 1979, 5: 17-37.

# Appendix A: Notation

| | | | |
|---|---|---|---|
| $h$ | Convective heat transfer coefficient | $R$ | Gas constant for air |
| $Bi$ | Biot number | $H, y$ | Driving head, height |
| $\lambda$ | Thermal conductivity | $g$ | Gravitational acceleration |
| $r$ | Radius, pressure ratio | $\eta$ | Efficiency |
| $q$ | Heat flux | $\gamma$ | Ratio of specific heats for air |
| $T$ | Temperature | $x$ | Volumetric ratio of air to water at the air inlet, see equation 7 |
| $c_p$ | Specific heat capacity at constant pressure | $k$ | Lumped pressure loss factor |
| $\rho$ | Density | $v$ | Velocity |
| $P, p$ | Pressure | $C_T$ | Pressure recovery coefficient |
| $W$ | Work | $\varphi$ | Diffuser included angle |
| $m$ | Mass flow rate | $L$ | Length |
| $\alpha$ | Void fraction | $D$ | Diameter |
| $\mu$ | Dynamic viscosity | | |

**Subscripts**

| | |
|---|---|
| *1* | aerator inlet level |
| *2* | siphon outlet (atmospheric pressure) surface level |
| *a* | air |
| *w* | water |
| *r* | relative (slip) |
| *up* | upstream |
| *mix* | mixture |